The Structure of the Virtual Photon†

Claudia Glasman*
representing the ZEUS Collaboration

*Department of Physics and Astronomy, Kelvin Building,
University of Glasgow, Glasgow, G12 8QQ, UK

Abstract. Measurements of dijet cross sections for virtual photons are presented as a function of x_γ^{OBS}, the fraction of the virtual photon energy invested in the production of the dijet system, using the ZEUS detector. Comparisons to QCD predictions show that a resolved photon component is needed to describe the data up to values of the photon virtuality comparable to the scale of the interaction.

INTRODUCTION

It has been long established that real photons have a partonic structure from measurements of the photon structure function F_2^γ in $e\gamma$ interactions [1] and observation of resolved photon processes in γp interactions [2] and of single- and double-resolved processes in $\gamma\gamma$ interactions [3]. Thus, it is natural to expect that virtual photons also have a partonic structure [4–7]. QCD predicts that the parton densities of virtual photons become logarithmically suppressed as the virtuality of the probed photon P^2 increases for fixed μ^2, the scale of the interaction; μ^2 is usually taken as Q^2 (Q^2 is the virtuality of the probing photon) in deep inelastic scattering (DIS) $e\gamma$ and the jet transverse energy (E_T^{jet}) in jet production.

The virtual photon structure function $F_2^{\gamma^*}$ at leading order (LO) in QCD is given by

$$F_2^{\gamma^*}(x_{\gamma^*}, P^2, \mu^2_{F_{\gamma^*}}) = \sum_q x_{\gamma^*}\ e_q^2\ [f_{q/\gamma^*}(x_{\gamma^*}, P^2, \mu^2_{F_{\gamma^*}}) + f_{\bar{q}/\gamma^*}(x_{\gamma^*}, P^2, \mu^2_{F_{\gamma^*}})],$$

where x_{γ^*} is the fraction of the virtual photon momentum taken by the interacting parton, $\mu^2_{F_{\gamma^*}}$ is the virtual photon fragmentation scale and e_q is the quark charge. The virtual photon quark densities f_{q/γ^*} contain two terms, as in the case of the real photon,

† Talk given at the *International Conference on the Structure and Interactions of the Photon* (PHOTON 2000), Ambleside, UK, August $26^{th} - 31^{st}$, 2000.

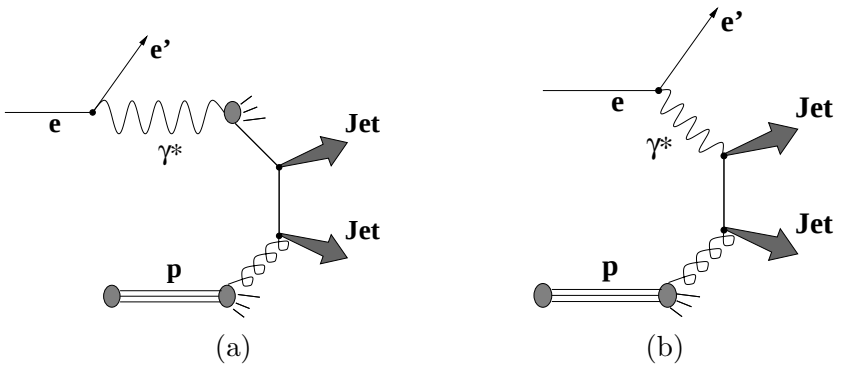

(a) (b)

FIGURE 1. (a) Resolved and (b) direct virtual-photon processes.

$$f_{i/\gamma^*}(x_{\gamma^*}, P^2, \mu^2_{F_{\gamma^*}}) = f^{\rm had}_{i/\gamma^*}(x_{\gamma^*}, P^2, \mu^2_{F_{\gamma^*}}) + f^{\rm anom}_{i/\gamma^*}(x_{\gamma^*}, P^2, \mu^2_{F_{\gamma^*}}),$$

one term associated to the non-perturbative hadronic component ($f^{\rm had}$) and a term $f^{\rm anom}$, unique to the photon, which expresses the direct coupling of the photon to a $q\bar{q}$ pair, calculable in perturbative QCD (pQCD). The hadronic component is the one expected to decrease as P^2 increases. The first measurements of the structure function of the virtual photon were done by PLUTO [8]. Only recently new measurements from LEP have become available [9].

At HERA, the virtual photon structure is studied in jet production mediated by virtual photons. In LO QCD, two processes are expected to contribute to the jet cross section: resolved processes (figure 1a) in which the virtual photon interacts with the proton via its hadronic component giving two jets in the final state, and the direct processes (figure 1b) in which the virtual photon interacts as a point-like particle with a parton from the proton.

The dijet production cross sections in LO QCD for direct and resolved processes are given by

$$\sigma_D^{LO,ep} = \int d\Omega \; f_{\gamma^*/e}(y, P^2) \; f_{j/p}(x_p, \mu^2_{F_p}) \; d\sigma(\gamma^* j \to \text{jet jet})$$

and

$$\sigma_R^{LO,ep} = \int d\Omega \; f_{\gamma^*/e}(y, P^2) \; f_{i/\gamma^*}(x_{\gamma^*}, P^2, \mu^2_{F_{\gamma^*}}) \; f_{j/p}(x_p, \mu^2_{F_p}) \; d\sigma(ij \to \text{jet jet}),$$

where the integrals are performed over the phase space represented by "$d\Omega$"; $f_{\gamma^*/e}(y, P^2)$ is the flux of virtual photons in the positron and y is the fraction of the positron energy taken by the virtual photon; $f_{j/p}(x_p, \mu^2_{F_p})$ are the parton densities in the proton and x_p is the fraction of the proton momentum taken by parton j; $\mu^2_{F_p}$ is the proton fragmentation scale; and $d\sigma(\gamma^*(i)j \to \text{jet jet})$ is the subprocess cross section, calculable in pQCD. In the case of resolved processes, there is an additional ingredient: the parton densities in the virtual photon $f_{i/\gamma^*}(x_{\gamma^*}, P^2, \mu^2_{F_{\gamma^*}})$,

for which up to the present there is only very little experimental information. This allows the study of the virtual photon structure by measuring jet cross sections.

The contribution to the dijet cross section from resolved processes is expected to decrease relative to the contribution from the direct processes as $P^2 \to \mu^2$; this means that the partonic content of the virtual photon becomes suppressed as P^2 increases. Experimentally, resolved and direct processes are separated by using the variable x_γ^{OBS},

$$x_\gamma^{OBS} = \frac{1}{2yE_e}(E_T^{jet1}e^{-\eta^{jet1}} + E_T^{jet2}e^{-\eta^{jet2}}), \tag{1}$$

where $\eta^{jet1,2}$ is the jet pseudorapidity and E_e is the positron beam energy. x_γ^{OBS} measures the fraction of the virtual photon energy invested in the production of the dijet system and it is well defined at all orders in pQCD. For resolved (direct) processes, x_γ^{OBS} takes low (high) values.

The measurements presented here were performed with the ZEUS detector at HERA. During 1995 to 1997 HERA operated with positrons of energy $E_e = 27.5$ GeV and protons of energy $E_p = 820$ GeV.

DIJET CROSS SECTIONS IN THE LABORATORY FRAME

The x_γ^{OBS} distribution displays a high sensitivity to the virtual photon structure. Figure 2 shows the x_γ^{OBS} distribution for a sample of dijet events in three regions of P^2. In all the P^2 regions studied, a significant resolved contribution is needed in the Monte Carlo to describe the data for $x_\gamma^{OBS} < 0.75$. Direct processes alone (the shaded area in figure 2) cannot describe the data [10].

Dijet cross sections as a function of x_γ^{OBS} have been measured for jets found using the longitudinally invariant k_T cluster algorithm in the inclusive mode [11]. The measurements have been performed in the kinematic region given by $0.2 < y < 0.55$ and in three regions of P^2: $P^2 \approx 0$ (the photoproduction regime in which the scattered positron is lost in the beam pipe, figure 3a), $0.1 < P^2 < 0.55$ GeV^2 (the intermediate P^2 region, in which the scattered positron is detected in the beam pipe calorimeter, figure 3b) and $1.5 < P^2 < 4.5$ GeV^2 (the low P^2 DIS regime, in which the scattered positron is detected in the uranium-scintillator calorimeter, figure 3c). The events are required to have at least two jets with $E_T^{jet} > 5.5$ GeV and $-1.125 < \eta^{jet} < 2.2$. The data show that the shape of the measured cross section changes markedly with increasing P^2: the cross section for low x_γ^{OBS} values decreases faster than at high x_γ^{OBS} values.

The measurements have been compared to several Monte Carlo models using various parametrisations of the photon parton densities (PDFs). The GRV [12] and WHIT2 [13] photon PDFs have been extracted for real photons and have no P^2 dependence. On the other hand, the SaS 1D [4] photon PDFs consist of

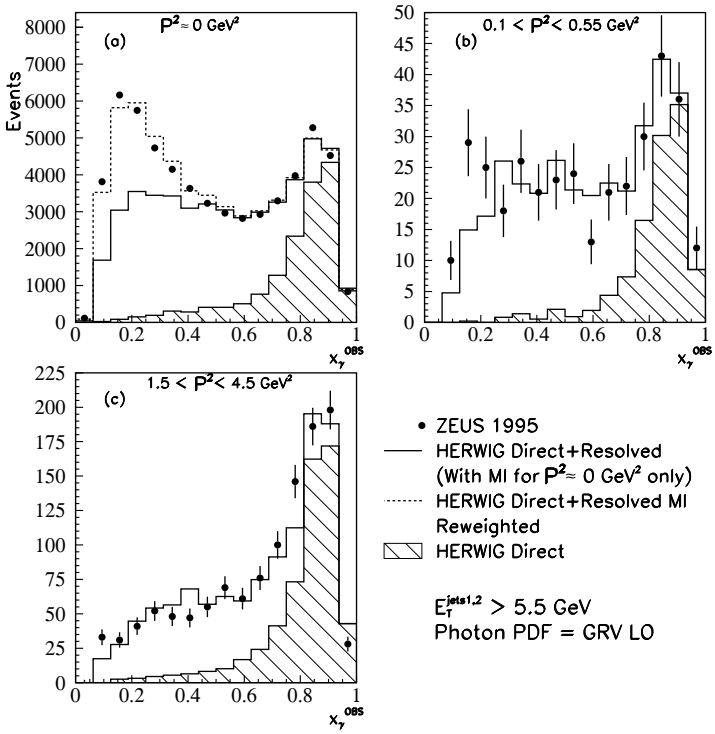

FIGURE 2. The uncorrected x_γ^{OBS} distribution (black dots). Monte Carlo simulations using HERWIG are shown for comparison.

two components with different P^2 dependence: the hadronic part decreases as $\approx (m_\rho^2/(m_\rho^2+P^2))^2$ with increasing P^2, while the P^2 dependence of the anomalous component goes like $\sim \log(\mu^2/P^2)$. The predictions of HERWIG [14] using the GRV PDFs do not describe the data, as expected since they have no P^2 dependence. The prediction based on WHIT2 provides a reasonable description of the data in the photoproduction and in the intermediate P^2 regimes. The predictions using SaS 1D agree with the data at high x_γ^{OBS} in all regimes. The DIS Monte Carlo LEPTO [15] is compared to the data in the DIS regime. It underestimates the data at low x_γ^{OBS}, i.e. parton shower effects are not the sole contribution to this region of x_γ^{OBS} and P^2.

The low E_T^{jet} region is affected by contributions from the presence of a possible underlying event, which may mask the P^2 evolution of the virtual photon. Therefore, measurements of the dijet cross sections have been performed at higher transverse energies. For these measurements, two jets were required with $E_T^{jet,1(2)} > 7.5(6.5)$ GeV and $-1.125 < \eta^{jet1,2} < 1.875$. The cross sections are shown in figure 4. At low x_γ^{OBS} the cross sections are also observed to decrease faster with P^2 than at high x_γ^{OBS}. The predictions from HERWIG based on the GRV PDFs are in good agreement with the data in the two lowest P^2 ranges, but fail at higher P^2. On the other hand, the predictions based on SaS 1D agree with the data at high P^2 but underestimate the data at low and intermediate P^2 at low x_γ^{OBS}. The predictions from LEPTO at high P^2 underestimate the data.

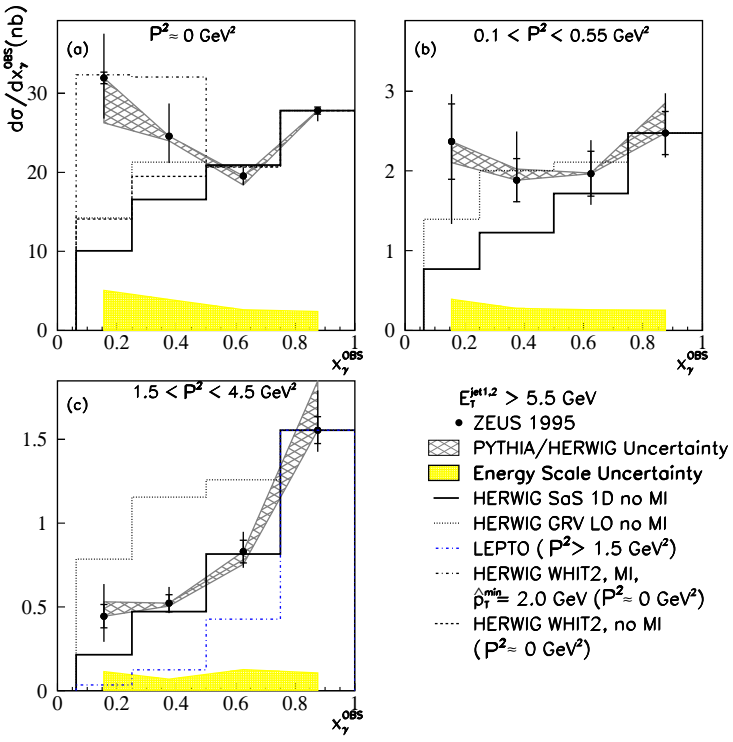

FIGURE 3. The measured dijet cross section $d\sigma/dx_\gamma^{OBS}$ (black dots) in the laboratory frame. The inner error bars represent the statistical errors of the data, and the outer error bars show the statistical errors and uncorrelated systematic uncertainties added in quadrature. The shaded band displays the uncertainty due to the absolute energy scale of the jets and the hatched band displays the uncertainty due to the modelling of the jet fragmentation. Monte Carlo calculations using HERWIG and LEPTO are shown for comparison.

The P^2 evolution of the virtual photon structure was studied further by measuring the ratio of the dijet cross section for $x_\gamma^{OBS} < 0.75$ (enriched in resolved processes) to the dijet cross section for $x_\gamma^{OBS} > 0.75$ (enriched in direct processes). The ratio (see figure 5) falls steeply with P^2 which may be interpreted as the suppression of the resolved photon component as the virtuality of the photon increases. The prediction of HERWIG based on the GRV PDFs is constant, as expected from a photon structure without P^2 dependence. The prediction of SaS 1D decreases with P^2 but lies below the data at low P^2 and the prediction from LEPTO shows that the contribution to the ratio from parton shower effects alone is not enough to explain the P^2 dependence of the data. QCD predictions have been calculated using the program JetViP [16] and different parametrisations of the photon PDFs. The predictions show sensitivity to the choice of PDF but lie well below the data. Hadronisation corrections ($\sim 20 - 30\%$) are insufficient to explain the discrepancy.

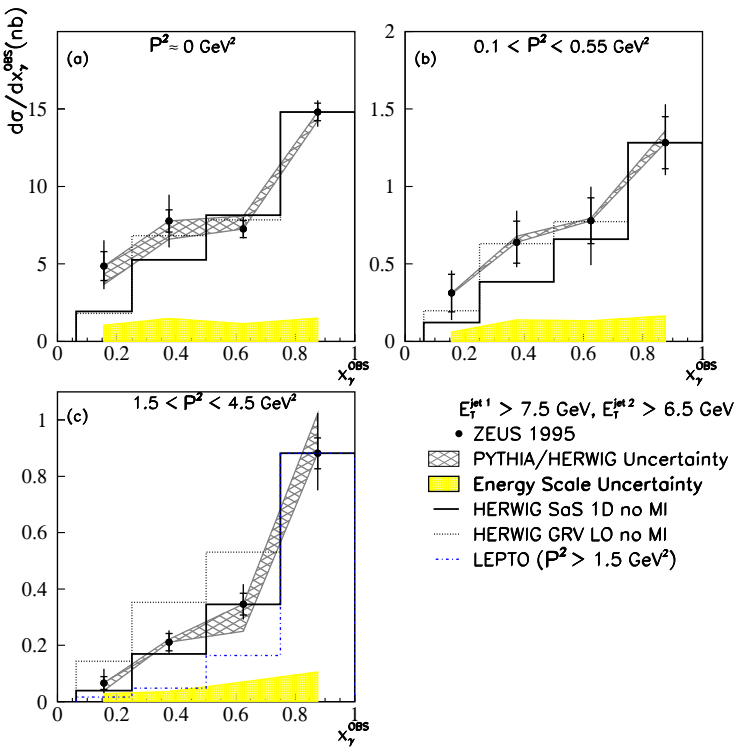

FIGURE 4. The measured dijet cross section $d\sigma/dx_\gamma^{OBS}$ (black dots) in the laboratory frame. Monte Carlo calculations using HERWIG and LEPTO are shown for comparison.

DIJET CROSS SECTIONS IN THE $\gamma^* p$ FRAME

For $P^2 \gg 0$, the definition of x_γ^{OBS} (equation 1) is still valid. However, the photon remnant may have high transverse energy in the laboratory frame and be considered as a jet. The solution to avoid this problem is to transform to the $\gamma^* p$ frame. In such a frame the photon remnant has very low transverse energy and will not be mistaken for a jet emanating from the hard interaction.

Figure 6a shows the measurements of the dijet cross section as a function of x_γ^{OBS} in the $\gamma^* p$ frame [17]. The measurements have been performed in the kinematic region given by $0.2 < y < 0.55$ and $0.1 < P^2 < 10^4$ GeV^2. The events are required to have at least two jets with $E_{T,\gamma^* p}^{jet1(2)} > 7.5(6.5)$ GeV and $-3 < \eta_{\gamma^* p}^{jet1,2} < 0$. Also for these measurements the shape of the measured cross section changes with increasing P^2: the cross section for low x_γ^{OBS} values falls more rapidly with increasing P^2 than at high x_γ^{OBS} values.

The predictions of HERWIG based on the SaS 1D PDFs (see figure 6a) give a good description of the data in the high P^2 region but fail in the intermediate P^2 region. A resolved photon component is needed to describe the data up to $P^2 \sim 49$ GeV^2. Above this value, the HERWIG prediction is dominated by the direct component and describes the data well. Therefore, for $P^2 \geq (E_T^{jet})^2$, direct processes alone are able to describe the data.

The ratio of the cross section for $x_\gamma^{OBS} < 0.75$ and $x_\gamma^{OBS} > 0.75$ also falls steeply

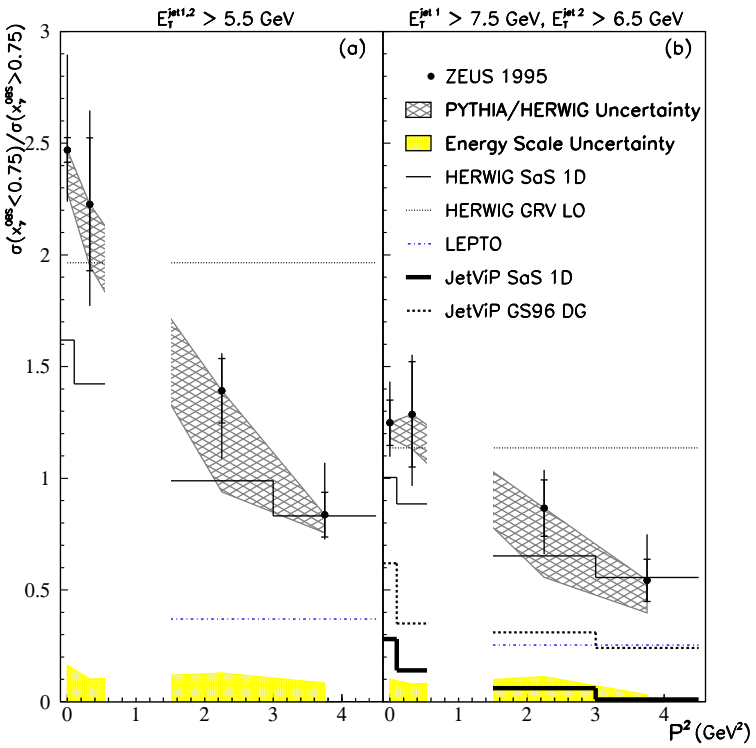

FIGURE 5. The ratio of dijet cross sections, $\sigma(x_\gamma^{OBS} < 0.75)/\sigma(x_\gamma^{OBS} > 0.75)$, as a function of P^2 (black dots). Monte Carlo (HERWIG and LEPTO) and QCD (JetVip) calculations are shown for comparison.

in the $\gamma^* p$ frame with increasing P^2 (figure 6b). The prediction of SaS 1D shows a decrease with P^2 but lies below the data in the whole P^2 range. The ratio of the data to the SaS 1D prediction (inset in figure 6b) has a constant value of ~ 1.3. This indicates that the resolved component suppression included in these PDFs is in agreement with the data, but they underestimate the fraction of resolved component by $\sim 30\%$.

SUMMARY AND CONCLUSIONS

Dijet cross sections as a function of x_γ^{OBS} have been measured in the laboratory and $\gamma^* p$ frames in the kinematic region given by $0.2 < y < 0.55$ and $0 \lesssim P^2 < 10^4$ GeV^2 for jets found using the longitudinally invariant k_T cluster algorithm in the inclusive mode. The x_γ^{OBS} dependence of the measured cross sections changes with increasing P^2: the cross section for low x_γ^{OBS} values decreases faster than at high x_γ^{OBS} values. The predictions of HERWIG based on the SaS 1D photon PDFs describe the data for $1.5 < P^2 < 10^4$ GeV^2 but fail in the region $0.1 < P^2 < 0.55$ GeV^2. A resolved photon component is needed to describe the data up to $P^2 \sim 49$ GeV^2, i.e. where the virtual photon is probed at a scale comparable to the hard interaction scale $(E_T^{jet})^2 \sim (7\text{ GeV})^2$. The ratio of the dijet cross section $\sigma(x_\gamma^{OBS} <$

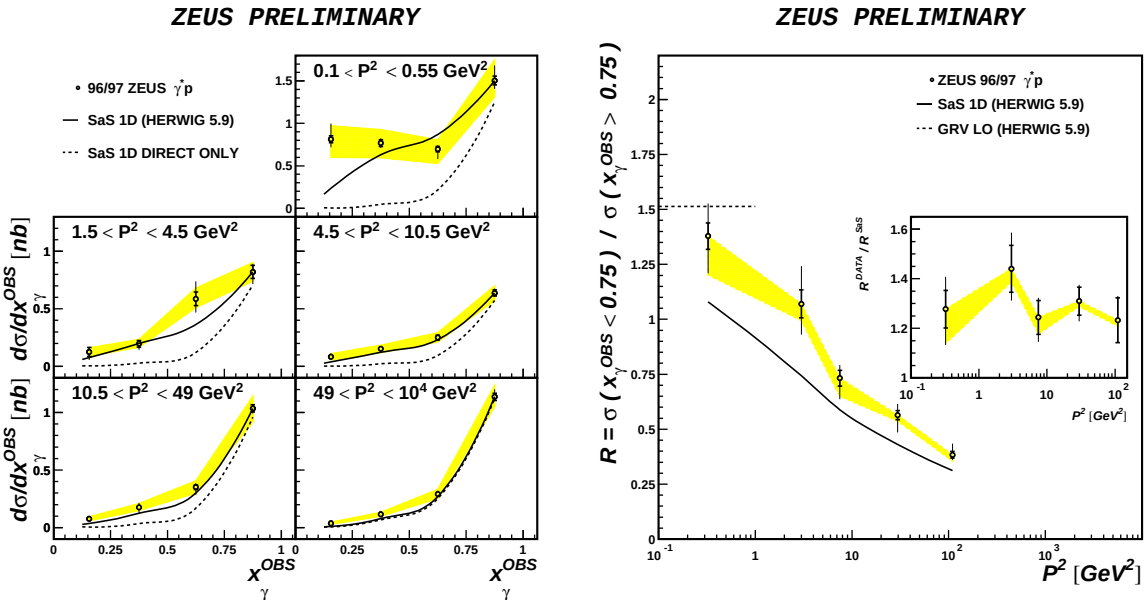

(a) (b)

FIGURE 6. (a) The measured dijet $d\sigma/dx_\gamma^{OBS}$ (black dots) in the $\gamma^* p$ frame. (b) The ratio of dijet cross sections, $\sigma(x_\gamma^{OBS} < 0.75)/\sigma(x_\gamma^{OBS} > 0.75)$, as a function of P^2 (black dots). Monte Carlo calculations using HERWIG are shown for comparison.

$0.75)/\sigma(x_\gamma^{OBS} > 0.75)$ decreases with P^2; the predicted P^2 dependence of the ratio agrees with the data, but it underestimates the fraction of the resolved component by $\sim 30\%$. This result can be interpreted in terms of a resolved photon component that is suppressed as the photon virtuality increases.

Acknowledgements. I would like to thank my colleagues from ZEUS for their help in preparing this report and the organisers of the conference for providing a warm atmosphere and hospitality.

REFERENCES

1. JADE Collaboration, W. Bartel *et al*, *Phys. Lett.* **B** 121 (1983) 203 and *Z. Phys.* **C** 24 (1984) 231; TASSO Collaboration, M. Althoff *et al*, *Z. Phys.* **C** 31 (1986) 527; PLUTO Collaboration, C. Berger *et al*, *Phys. Lett.* **B** 107 (1981) 168, *Phys. Lett.* **B** 142 (1984) 111 and *Nucl. Phys.* **B** 281 (1987) 365; OPAL Collaboration, R. Akers *et al*, *Z. Phys.* **C** 61 (1994) 199, K. Ackerstaff *et al*, *Phys. Lett.* **B** 411 (1997) 387, *Phys. Lett.* **B** 412 (1997) 225, *Z. Phys.* **C** 74 (1997) 33 and G. Abbiendi *et al*, submitted to *Eur. Phys. Jour.* **C**, hep-ex/0007018; L3 Collaboration, M. Acciarri *et al*, *Phys. Lett.* **B** 436 (1998) 403, *Phys. Lett.* **B** 447 (1999) 147 and *Phys. Lett.* **B** 483 (2000)

373; ALEPH Collaboration, R. Barate *et al*, *Phys. Lett.* **B** 458 (1999) 152; DELPHI Collaboration, P. Abreu *et al*, *Z. Phys.* **C** 69 (1996) 223.
2. ZEUS Collaboration, M. Derrick *et al*, *Phys. Lett.* **B** 297 (1992) 404, *Phys. Lett.* **B** 322 (1994) 287, *Phys. Lett.* **B** 342 (1995) 417, *Phys. Lett.* **B** 348 (1995) 665, *Phys. Lett.* **B** 354 (1995) 163, *Phys. Lett.* **B** 384 (1996) 401, J. Breitweg *et al*, *Phys. Lett.* **B** 443 (1998) 394, *Eur. Phys. Jour.* **C** 1 (1998) 109, *Eur. Phys. Jour.* **C** 4 (1998) 591 and *Eur. Phys. Jour.* **C** 11 (1999) 35; H1 Collaboration, T. Ahmed *et al*, *Phys. Lett.* **B** 297 (1992) 205, I. Abt *et al*, *Phys. Lett.* **B** 314 (1993) 436, T. Ahmed *et al*, *Nucl. Phys.* **B** 445 (1995) 195, S. Aid *et al*, *Z. Phys.* **C** 70 (1996) 17, C. Adloff *et al*, *Eur. Phys. Jour.* **C** 1 (1998) 97, *Eur. Phys. Jour.* **C** 10 (1999) 363, *Phys. Lett.* **B** 483 (2000) 36 and *Eur. Phys. Jour.* **C** 13 (2000) 397.
3. JADE Collaboration, W. Bartel *et al*, *Phys. Lett.* **B** 107 (1981) 163; TASSO Collaboration, R. Brandelik *et al*, *Phys. Lett.* **B** 107 (1981) 290 and M. Althoff *et al*, *Phys. Lett.* **B** 138 (1984) 219; PLUTO Collaboration, C. Berger *et al*, *Z. Phys.* **C** 26 (1984) 191, *Z. Phys.* **C** 29 (1985) 499 and *Z. Phys.* **C** 33 (1987) 351; OPAL Collaboration, K. Ackerstaff *et al*, *Z. Phys.* **C** 73 (1997) 433 and G. Abbiendi *et al*, *Eur. Phys. Jour.* **C** 10 (1999) 547.
4. G. Schuler and T. Sjöstrand, *Phys. Lett.* **B** 376 (1996) 193.
5. M. Drees and R. Godbole, *Phys. Rev.* **D** 50 (1994) 3124.
6. T. Uematsu and T. Walsh, *Phys. Lett.* **B** 101 (1981) 263 and *Nucl. Phys.* **B** 199 (1982) 93; F. Borzumati and G. Schuler, *Z. Phys.* **C** 58 (1993) 139; M. Glück, E. Reya and I. Schienbein, *Phys. Rev.* **D** 60 (1999) 54019.
7. M. Glück, E. Reya and M. Stratmann, *Phys. Rev.* **D** 54 (1996) 5515; D. de Florian, C. Canal and R. Sassot, *Z. Phys.* **C** 75 (1997) 265; M. Klasen, G. Kramer and B. Pötter, *Eur. Phys. Jour.* **C** 1 (1998) 261.
8. PLUTO Collaboration, C. Berger *et al*, *Phys. Lett.* **B** 142 (1984) 119.
9. L3 Collaboration, M. Acciarri *et al*, *Phys. Lett.* **B** 438 (1998) 363.
10. ZEUS Collaboration, J. Breitweg *et al*, *Phys. Lett.* **B** 479 (2000) 37.
11. S. Catani *et al*, *Nucl. Phys.* **B** 406 (1993) 187; S.D. Ellis and D.E. Soper, *Phys. Rev.* **D** 48 (1993) 3160; M.H. Seymour, *Nucl. Phys.* **B** 513 (1998) 269.
12. M. Glück, E. Reya and A. Vogt, *Phys. Rev.* **D** 46 (1992) 1973.
13. K. Hagiwara, M. Tanaka and I. Watanabe, *Phys. Rev.* **D** 51 (1995) 3197.
14. G. Marchesini *et al*, *Comp. Phys. Comm.* 67 (1992) 465.
15. G. Ingelman, A. Edin and J. Rathsman, *Comp. Phys. Comm.* 101 (1997) 108.
16. G. Kramer and B. Pötter, *Eur. Phys. Jour.* **C** 5 (1998) 665; B. Pötter, *Eur. Phys. Jour. direct* **C** 5 (1999) 1 and *Comp. Phys. Comm.* 119 (1999) 4.
17. ZEUS Collaboration, "Measurements of the Structure of Virtual Photons", paper 426, submitted to the XXXth International Conference on HEP, Osaka (2000).